UCLA
COMPUTATIONAL AND APPLIED MATHEMATICS

Stability of Interpolation on Overlapping Grids

Fredrik Olsson
N. Anders Petersson

November 1994

CAM Report 94-35

Department of Mathematics
University of California, Los Angeles
Los Angeles, CA. 90024-1555

Stability of Interpolation on Overlapping Grids

Fredrik Olsson [1] N. Anders Petersson [2]

November 23, 1994

[1]Center for Computational Mathematics and Mechanics, Royal Institute of Technology, Stockholm, and Swedish Pulp and Paper Research Institute, Stockholm, Sweden,
[2]Department of Mathematics, UCLA, Los Angeles, CA 90024, USA.

Abstract

The stability of interpolation for one-dimensional overlapping grids is considered. The Cauchy-problem for a second order accurate centered finite difference approximation of $u_t = u_x$ is analyzed on the semi-discrete level. The existence of generalized eigenvalues is demonstrated for some rare overlap parameters, in which cases the discretization is found to be unstable. It is demonstrated that the stability can be recovered by adding artificial dissipation to the equation. Numerical experiments on the strip problem show that when a second order dissipation is used, the amount of dissipation necessary to cancel the spurious growth is $O(h^2)$ in the absence of generalized eigenvalues and $O(h)$ in their presence, where h is the grid size. It is also demonstrated that the accuracy is improved by using a fourth order dissipation.

Keywords: overlapping grid, GKS-stability, artificial dissipation.

AMS classifications: 65M12 (primary), 65M06, 65M55.

1 Introduction

When finite differences are used to numerically solve partial differential equations, the mesh must be structured as opposed to unstructured meshes used with finite elements or finite volume techniques. The advantage with a structured mesh is that it is easier to construct an efficient numerical algorithm. The apparent disadvantage is the difficulty to construct structured meshes for complicated geometries. One successful solution to this problem is to use overlapping composite meshes. Then the region is divided into subregions, each of which can be discretized with a structured mesh. Instead of patching the subregions along common boundaries they overlap and each subregion can be changed independently of the others, something which further facilitates the construction of the meshes. Additional boundary conditions must be given for the new sub-domain boundaries in the interior of the original domain. The values at the boundary are interpolated from the interior of an overlapping neighboring mesh. It is the influence of these added "boundary conditions" on the stability of the numerical solution that is to be studied in this paper.

We will consider the wave equation

$$\begin{aligned} u_t &= u_x, \quad t \geq 0, \quad x \in \Omega_k \subseteq \mathbf{R}, \quad k = 1, 2, \\ u(0,x) &= f(x), \quad \int_{\Omega_k} |f(x)|^2 \, dx < \infty, \end{aligned} \tag{1}$$

for the Cauchy problem $\Omega_1 =: \{x : -\infty < x < +\infty\}$ and the strip problem $\Omega_2 =: \{x : 0 \leq x \leq 2\pi\}$ with in/outflow boundary conditions. Since we want to see the effect on the stability of the interpolation between the two meshes without making any assumptions about the time integration, the analysis is done on the semi-discrete problem where only the space variable is discretized. In both cases we treat two grids with one overlap region, see the schematic picture in figure 1.

Our analysis is an application of the normal mode techniques developed by Gustafsson, Kreiss and Sundström [6] and described in more detail in Gustafsson, Kreiss and Oliger [5]. There are many applications of the normal mode technique in the literature. Reyna [10] analyzed the semi-discrete Cauchy-problem for an overlapping grid and Starius [11] did a similar analysis for the fully discretized (Lax-Wendroff) half-plane problem. More recently, Pärt–Enander and Sjögreen [9] analyzed the fully discrete problem to determine stability properties of different interpolation methods. Similar techniques have also been used by Berger [1] and Ciment [3, 4] to study stability of interfaces with mesh refinement. Necessary and sufficient conditions for stability of the semi-discrete strip problem discretized on one grid was reported by Strikwerda [12]. For a more physical interpretation of the stability theory for one grid, we refer to the work by Trefethen [13].

In section 2 we will state some well-known results from the normal mode theory developed in [5]. We present the Kreiss condition, which together with some additional assumptions is sufficient to ensure stability of general difference approximations in the presence of a boundary. We also state a lemma that relates the Kreiss condition to algebraic conditions for an eigenvalue problem corresponding to the difference approximation. We thereafter present a lemma that in essence says that when two half-plane problems

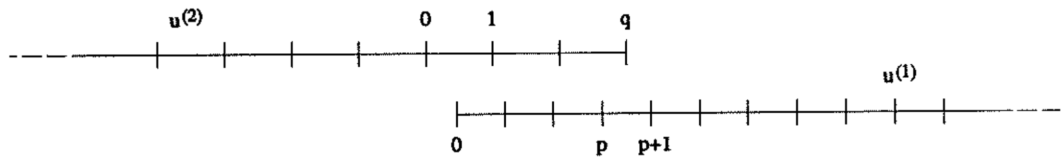

Figure 1: Schematic picture of an one-dimensional overlapping grid.

are combined into a strip problem, the resulting system will be stable if the two half-plane problems were stable. We want to emphasize that the theory is based on a stability criterion which does not exclude exponential growth as long as it is bounded independently of the data and the grid spacing h. This point will be discussed more below.

In section 3 we study (1) for the Cauchy problem discretized in space by second order accurate centered differences on two overlapping grids as is shown in figure 1. Grid 1, for $x \geq x_0^{(1)}$, has grid spacing h_1 and grid 2, for $x \leq h_2(q-\alpha)+x_0^{(1)}$, has grid spacing h_2. Introduce the grid functions $u_j^{(1)}$ and $u_j^{(2)}$ for the left and right grid respectively:

$$\begin{aligned} u_j^{(1)}(t) &\approx u(t, jh_1 + x_0^{(1)}), && j = 0, 1, \ldots, \\ u_j^{(2)}(t) &\approx u(t, (j-\alpha)h_2 + x_0^{(1)}), && j = q, q-1, \ldots, \quad 0 \leq \alpha < 1. \end{aligned}$$

To apply the theory from section 2, it is convenient to view the discretization of the Cauchy problem on an overlapping grid as a half-plane problem for a system of two equations for $(u^{(1)}, u^{(2)})^T$ coupled by the interpolation relations as boundary conditions. We will in the following call this system the interpolation problem. We will show that for some overlaps, the corresponding eigenvalue problem has generalized eigenvalues. The Kreiss condition is therefore not fulfilled and we cannot determine stability from the algebraic conditions. However, these unwanted eigensolutions disappear by changing the overlap by an arbitrarily small amount, e.g. by shifting one grid slightly.

By adding a viscous term νu_{xx} to the right hand side of the wave equation (1), and discretizing space by second order accurate centered differences, we will in section 4 prove that the viscous interpolation problem is stable for all $\nu > 0$ regardless of the interpolation parameters at the overlap.

In section 5 we investigate the stability of the strip problem, which can be thought of as an initial boundary value problem for $(u^{(1)}, u^{(2)})^T$ where at one boundary we have the interpolation conditions and at the other boundary we have an inflow boundary condition for one component and an outflow condition for the other. By using the theory of section 2, we know that the strip problem is stable if both the left and right half-plane problems are stable. It is not difficult to show that the half-plane problem with the in/outflow boundary conditions is stable. We therefore know that the stability of the strip problem is determined by the stability of the interpolation problem.

Using the same spatial discretization as in the analysis and the classical fourth order Runge–Kutta method to integrate the solution in time, we will calculate numerical solutions of (1) for the strip problem. By computing the solution for large times with an overlap that does not give generalized eigenvalues for the inviscid interpolation problem, we are able to see the exponential growth, which corresponds accurately to the growth predicted in the eigenvalue analysis of the strip problem. This type of growth, which is very weak, is not an instability according to our definition. It is a result of the spurious modes which always are present because of the discretization. The examples show that the growth rate will decrease with grid refinement and increase when the overlap is moved closer to the boundary. This is explained by the spatial decay of the spurious modes. In contrast, when we solve the strip problem with overlaps that give generalized eigenvalues for the inviscid interpolation problem, we see a stronger spurious growth where the growth rate increases with mesh refinement. This latter type of growth represents an instability according to our definition.

According to the previously described analysis, the strip problem becomes stable for all overlap parameters if a second order dissipative term $\nu D_+ D_- u_j$, $\nu > 0$, is added to the discretized equation. Here, D_+ and D_- denote the standard forward and backward divided difference operators. However, the solution can grow exponentially in time but the growth rate is bounded independently of the grid spacing h. If we are interested in solving the inviscid wave equation, we want ν to decay with h for accuracy reasons. When the inviscid interpolation problem is stable, the amount of viscosity necessary to obtain a solution of the strip problem without spurious growth is found to be $\nu \sim O(h^2)$. However, in the cases where the corresponding interpolation problem has a generalized eigenvalue on the imaginary axis, the amount of viscosity is found to be $\nu \sim O(h)$. Thus, in the absence of the generalized eigenvalues, the method is still second order accurate with respect to the inviscid equation, but when generalized eigenvalues are present, the method is only first order accurate. To cure the accuracy problem, we replace the second order dissipation term by the fourth order term $-\nu D_+^2 D_-^2 u_j$. It is found that this term damps the growing mode much more efficiently. Now, $\nu \sim O(h^3)$ is sufficient to cancel the spurious growth, even in the presence of generalized eigenvalues in the corresponding interpolation problem.

2 Sufficient Conditions for Stability

In this section we will state some well-known results from the normal mode theory presented in [5]. We will exemplify the ideas on the semi-discrete approximation of the half-plane problem for a hyperbolic system. We define a grid by $x_j = hj$, $j = 0, 1, 2, \ldots$, and denote a grid function with m vector components by $\bar{v}_j(t) \approx \bar{v}(x_j, t)$. Let us denote the k'th component of $\bar{v}_j$ by $v_j^{(k)}$ and define the scalar product and norm by

$$(\bar{v}, \bar{w})_h = (\bar{v}, \bar{w})_{1,\infty}, \quad \|\bar{v}\|_h^2 = (\bar{v}, \bar{v})_h, \quad \left|\bar{v}_j\right|^2 = \langle \bar{v}_j, \bar{v}_j \rangle,$$

where

$$(\bar{v}, \bar{w})_{r,s} = h \sum_{j=r}^{s} \langle \bar{v}_j, \bar{w}_j \rangle, \quad \langle \bar{v}_j, \bar{w}_j \rangle = \sum_{k=1}^{m} \left(v_j^{(k)}\right)^* w_j^{(k)}.$$

We denote the difference approximation by

$$\begin{aligned}
\frac{\partial \bar{v}_j(t)}{\partial t} &= Q\bar{v}_j(t) + \bar{F}_j(t), \quad j = 1,2,\ldots, \quad t \geq 0, \\
\bar{v}_j(0) &= 0, \qquad\qquad\qquad j = 1,2,\ldots, \\
L_0 \bar{v}_0(t) &= \bar{g}(t), \qquad\qquad\quad t \geq 0,
\end{aligned} \tag{2}$$

where $\sup_t \|\bar{F}(t)\|_h < \infty$ and $\sup_t |\bar{g}(t)| < \infty$. Here, L_0 is the boundary condition operator and the spatial difference operator Q has the form

$$Q = \frac{1}{h} \sum_{\nu=-r}^{p} B_\nu E^\nu,$$

where E is the shift operator and B_{-r} and B_p are non-singular matrices. The assumption that the initial data is homogeneous is not a restriction but is motivated by the use of the Laplace transform method to analyse the stability. A problem with inhomogeneous initial data $\bar{v}_j(0) = \bar{f}_j$ can be transformed to a problem with homogeneous initial data by the change of variables $\tilde{v}_j(t) = \bar{v}_j(t) - q(t)\bar{f}_j$, where $q(t)$ is a smooth function with $q(0) = 1$.

We define the Laplace-transform by

$$\hat{v}_j(s) = \int_0^\infty e^{-st} \bar{v}_j(t)\, dt, \quad s = i\xi + \eta, \quad \eta > 0.$$

When $\bar{F} \equiv 0$, the Laplace-transformed half-plane problem is

$$\begin{aligned}
\tilde{s}\hat{v}_j &= hQ\hat{v}_j \quad j = 1,2,\ldots, \quad \tilde{s} = hs, \\
L_0 \hat{v}_0 &= \hat{g}.
\end{aligned} \tag{3}$$

We make the following definition.

Definition 1 (The Kreiss condition) *Assume that there is a constant K independent of $\tilde{s}$ and $\hat{g}$ such that the solution of (3) satisfies*

$$\sum_{\nu=-r+1}^{p} |\hat{v}_\nu|^2 \leq K|\hat{g}|^2, \quad Re(\tilde{s}) > 0.$$

Then we say that the Kreiss condition is satisfied.

The stability properties of (2) are closely related to the eigenvalue problem:

$$\begin{aligned}
\tilde{s}\bar{\phi}_j &= hQ\bar{\phi}_j \quad j = 1,2,\ldots, \\
L_0 \bar{\phi}_0 &= 0.
\end{aligned} \tag{4}$$

We call $\tilde{s}$ an eigenvalue if there is a non-trivial solution $\bar{\phi}_j$ with $\mathrm{Re}(\tilde{s}) \geq 0$ and $\|\bar{\phi}\|_h < \infty$. In addition, if there is a solution with $\|\bar{\phi}\|_h = \infty$ on the imaginary axis $\mathrm{Re}(\tilde{s}) = 0$, we call $\tilde{s}$ a generalized eigenvalue. The Kreiss condition can be translated to algebraic conditions on the eigenvalue problem (4). One can prove:

Lemma 1 *The Kreiss condition is satisfied if and only if there are no eigenvalues or generalized eigenvalues for* $Re(\tilde{s}) \geq 0$.

Several stability definitions for difference approximations are possible and we refer to [5] for a discussion. Here we will call the difference approximation (2) stable if it satisfies the following criterion.

Definition 2 (Strong stability) *We say that the approximation (2) is strongly stable if*

$$\|\bar{v}(t)\|_h^2 \leq K e^{\delta t} \int_0^t \left(\|\bar{F}(\tau)\|_h^2 + |\bar{g}(\tau)|^2 \right) d\tau.$$

Here, K and δ are constants which do not depend on $\bar{F}$, $\bar{g}$, or h.

The stability investigation that we will perform in the present paper relies on the following theorem which is proven in [5].

Theorem 1 *Assume that $r \geq p$, that the Kreiss condition is satisfied and that the difference operator Q is semi-bounded for the Cauchy-problem, i.e. the coefficient matrices B_ν are Hermitian and*

$$Re(\bar{w}, Q\bar{w})_{-\infty,\infty} \leq 0, \qquad \text{for all} \quad \|\bar{w}\|_{-\infty,\infty} < \infty.$$

Then the approximation (2) is strongly stable.

We remark that the Kreiss condition is not a necessary condition for stability and the border-line case when there is an eigenvalue or generalized eigenvalue on the imaginary axis, $\text{Re}(s) = 0$, is very subtle. The difference approximation can be stable or unstable depending on the multiplicity of the eigenvalue and the boundedness of the corresponding eigenfunction, cf. [5] for details.

To determine the stability of the difference approximation for a bounded region, e.g. the strip problem $x \in \Omega_2 = \{x \mid 0 \leq x \leq 2\pi\}$, it is sufficient to establish stability for the right half-plane problem ($x \geq 0$) and the corresponding left half-plane problem ($x \leq 2\pi$), and use the following lemma which also is proven in [5].

Lemma 2 *The approximation of the strip problem is strongly stable if the operator Q is semi-bounded for the Cauchy-problem and the right and left half-plane problems are strongly stable.*

Even if the solutions of both half-plane problems do not grow in time it is possible that their combination into a strip problem has a solution which grows exponentially. An example of this situation is the combination of an energy feeding (inflow) boundary and a reflecting boundary. The boundary conditions can cause the solution of the strip problem to grow exponentially since the energy fed into the system by the inflow boundary condition gets reflected at the other boundary. The exponential growth can also be caused by the discretization beacause there is always a spurious mode present in the numerical solution. For these reasons, we can only expect to get strong stability with $\delta > 0$ for the strip problem. The second type of of growth is very weak and is usually only detected if the equation is integrated for a long time. If the growth causes problems, it can be compensated for by introducing a dissipative term in the equation, e.g. $\nu\partial^2 v/\partial x^2$. We remark that the difference approximation can be modified in other ways to make the strip problem stable with $\delta = 0$, cf. Paik [8].

In the follwing sections, we will apply the stability theory to a difference approximation of (1) on an overlapping grid. Instead of checking the Kreiss condition, we will use Lemma 1 and investigate the algebraic properties of the eigenvalue problem corresponding to (4).

3 The Inviscid Interpolation Problem

In this section, we will analyze the stability properties of (1) for the Cauchy problem discretized on two overlapping grids as is shown in figure 1. We approximate $\partial/\partial x$ with second order accurate centered differences. The semi-discrete version of the Cauchy problem (1) then becomes

$$\begin{aligned}
\frac{\partial u_j^{(1)}}{\partial t} &= \frac{u_{j+1}^{(1)} - u_{j-1}^{(1)}}{2h_1}, \qquad && j = 1, 2, \ldots, \quad t \geq 0, \\
u_j^{(1)}(0) &= f_j^{(1)}, && j = 1, 2, \ldots, \\
\frac{\partial u_j^{(2)}}{\partial t} &= \frac{u_{j+1}^{(2)} - u_{j-1}^{(2)}}{2h_2}, && j = q-1, q-2, \ldots, \quad t \geq 0, \\
u_j^{(2)}(0) &= f_j^{(2)}, && j = q-1, q-2, \ldots, \\
\|f^{(k)}\|_{h_k} &< \infty, && k = 1, 2,
\end{aligned} \tag{5}$$

augmented by the interpolation relations

$$\begin{aligned}
u_0^{(1)} &= (1-\alpha)u_0^{(2)} + \alpha u_1^{(2)}, \qquad && 0 \leq \alpha < 1, \\
u_q^{(2)} &= (1-\beta)u_p^{(1)} + \beta u_{p+1}^{(1)}, && 0 \leq \beta < 1.
\end{aligned} \tag{6}$$

The inhomogeneous initial data can be transformed into a forcing as was described in the previous section. We will in the following assume that this has already been done. To write the system in the form (2), we can take $h = h_1$, introduce a new variable

$$\bar{w}_j =: \begin{pmatrix} w_j^{(1)} \\ w_j^{(2)} \end{pmatrix} = \begin{pmatrix} u_j^{(1)} \\ u_{q-j}^{(2)} \end{pmatrix},$$

and write the system (5), (6) as

$$\begin{aligned}
\frac{d\bar{w}_j(t)}{dt} &= \begin{pmatrix} 1 & 0 \\ 0 & -h_1/h_2 \end{pmatrix} \frac{\bar{w}_{j+1} - \bar{w}_{j-1}}{2h} + \bar{F}_j(t), \quad j = 1, 2, \ldots, \quad t \geq 0, \\
\bar{w}_j(0) &= 0, \quad j = 1, 2, \ldots, \\
L_0 \bar{w}_0(t) &= 0, \quad t \geq 0.
\end{aligned} \tag{7}$$

The boundary condition operator is

$$L_0\bar{w}_0 =: \bar{w}_0 - \begin{pmatrix} 0 & 0 \\ 0 & \alpha \end{pmatrix} \bar{w}_{q-1} - \begin{pmatrix} 0 & 0 \\ 0 & 1-\alpha \end{pmatrix} \bar{w}_q - \begin{pmatrix} 1-\beta & 0 \\ 0 & 0 \end{pmatrix} \bar{w}_p - \begin{pmatrix} \beta & 0 \\ 0 & 0 \end{pmatrix} \bar{w}_{p+1}.$$

As was shown in the previous section, the stability of (7) is determined by the properties of the eigenvalue problem corresponding to (4):

$$\begin{aligned} hs\bar{\phi}_j &= \begin{pmatrix} 1 & 0 \\ 0 & -h_1/h_2 \end{pmatrix} \frac{\bar{\phi}_{j+1} - \bar{\phi}_{j-1}}{2}, \quad j = 1, 2, \ldots, \\ L_0\bar{\phi}_0 &= 0. \end{aligned} \tag{8}$$

The main result of this section is

Lemma 3 *Let $p \geq 1$ and $q \geq 2$. There are no eigenvalues of (8) in $Re(s) \geq 0$ and there are generalized eigenvalues on $Re(s) = 0$ if and only if*

$$\beta = 0 \quad \textit{and} \quad p = 2, 4, 6, \ldots,$$

or

$$\alpha = \beta = 0 \quad \textit{and} \quad p \neq q \quad \textit{and} \quad p \geq 3.$$

Instead of analyzing (8) we find it more convenient to change back to the notation of (5), i.e.

$$\bar{\phi}_j =: \begin{pmatrix} \phi_j^{(1)} \\ \phi_j^{(2)} \end{pmatrix} = \begin{pmatrix} \hat{y}_j^{(1)} \\ \hat{y}_{q-j}^{(2)} \end{pmatrix}.$$

This leads to the equivalent eigenvalue problem

$$\begin{aligned} 2sh_1\hat{y}_j^{(1)} &= \hat{y}_{j+1}^{(1)} - \hat{y}_{j-1}^{(1)}, & j &= 1, 2, \ldots, \\ 2sh_2\hat{y}_j^{(2)} &= \hat{y}_{j+1}^{(2)} - \hat{y}_{j-1}^{(2)}, & j &= q-1, q-2, \ldots, \\ \hat{y}_0^{(1)} &= (1-\alpha)\hat{y}_0^{(2)} + \alpha\hat{y}_1^{(2)}, \\ \hat{y}_q^{(2)} &= (1-\beta)\hat{y}_p^{(1)} + \beta\hat{y}_{p+1}^{(1)}. \end{aligned} \tag{9}$$

The general solution of the difference equation (9) can be written

$$\begin{aligned} \hat{y}_j^{(1)} &= \sigma_1\kappa_1^j + \sigma_2\kappa_2^j, & j &= 0, 1, \ldots, \\ \hat{y}_j^{(2)} &= \tau_1\lambda_1^{j-q} + \tau_2\lambda_2^{j-q}, & j &= q, q-1, \ldots, \end{aligned} \tag{10}$$

where κ_k, λ_k are the roots to the characteristic equations obtained by inserting (10) into the difference approximation (9), i.e.

$$\begin{aligned} 2\tilde{s}_1\kappa &= \kappa^2 - 1, & \tilde{s}_1 &= h_1 s, \\ 2\tilde{s}_2\lambda &= \lambda^2 + 1, & \tilde{s}_2 &= h_2 s. \end{aligned} \tag{11}$$

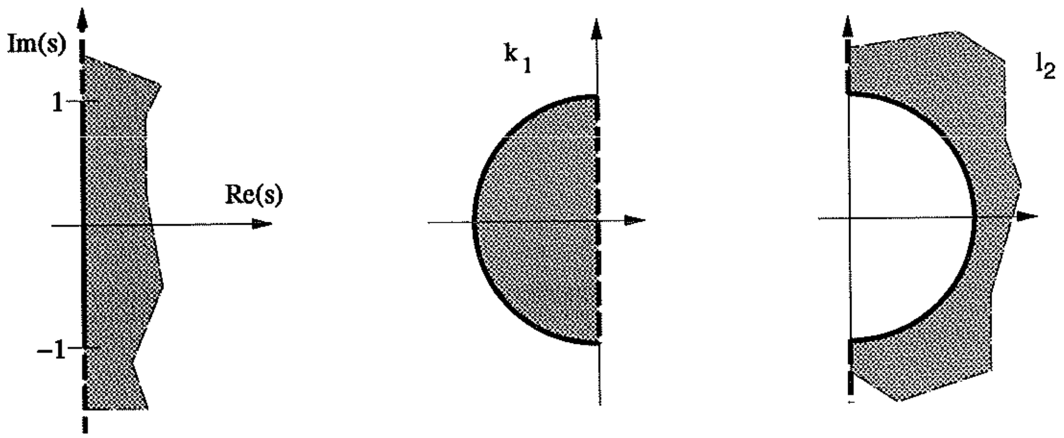

Figure 2: The functions $\kappa_1(s)$ and $\lambda_2(s)$ for the invicid case.

Thus,

$$\begin{aligned} \kappa_1(\tilde{s}_1) &= \tilde{s}_1 - \sqrt{1+\tilde{s}_1^2}, \quad \kappa_2(\tilde{s}_1) = \tilde{s}_1 + \sqrt{1+\tilde{s}_1^2}, \\ \lambda_1(\tilde{s}_2) &= \tilde{s}_2 - \sqrt{1+\tilde{s}_2^2}, \quad \lambda_2(\tilde{s}_2) = \tilde{s}_2 + \sqrt{1+\tilde{s}_2^2}, \end{aligned} \tag{12}$$

where

$$-\frac{\pi}{2} \leq \arg\sqrt{1+\tilde{s}_k^2} \leq \frac{\pi}{2}, \text{ for } \mathrm{Re}(\tilde{s}_k) \geq 0, \quad k = 1,2.$$

We note that $\lambda_1 = -1/\lambda_2$. Straightforward calculations, which are presented graphically in figure 2, give Lemma 4.

Lemma 4 *Consider the functions*

$$\begin{aligned} \kappa_1(\tilde{s}) &= \tilde{s} - \sqrt{1+\tilde{s}^2}, \\ \lambda_2(\tilde{s}) &= \tilde{s} + \sqrt{1+\tilde{s}^2}, \end{aligned}$$

where

$$-\frac{\pi}{2} \leq arg\sqrt{1+\tilde{s}^2} \leq \frac{\pi}{2}, \quad \textit{for } Re(\tilde{s}) \geq 0.$$

The function $\kappa_1(\tilde{s})$ maps the right half-plane $Re(\tilde{s}) \geq 0$ one-to-one onto the left half-disc $D_l := \{\kappa_1, |\kappa_1| \leq 1, Re(\kappa_1) \leq 0\}$. The function $\lambda_2(\tilde{s})$ maps the right half-plane $Re(\tilde{s}) \geq 0$ one-to-one onto the exterior of the right half-disc $\bar{D}_r := \{\lambda_2, |\lambda_2| \geq 1, Re(\lambda_2) \geq 0\}$. Furthermore, the function $\lambda_2^{-1}(\tilde{s}) = -\kappa_1(\tilde{s})$ maps the right half-plane $Re(\tilde{s}) \geq 0$ one-to-one onto the right half-disc $D_r := \{\lambda_2^{-1}, |\lambda_2^{-1}| \leq 1, Re(\lambda_2^{-1}) \geq 0\}$.

The solution (10) is bounded in space only if

$$\sigma_2 = \tau_1 = 0.$$

The interpolation conditions at the boundary give a linear system for σ_1 and τ_2:

$$\begin{pmatrix} 1 & -\left((1-\alpha)\lambda_2^{-1}+\alpha\right)\lambda_2^{1-q} \\ -\left(1-\beta+\beta\kappa_1\right)\kappa_1^p & 1 \end{pmatrix}\begin{pmatrix} \sigma_1 \\ \tau_2 \end{pmatrix} = 0. \tag{13}$$

There are no non-trivial solutions as long as the determinant

$$\Delta =: 1-\left((1-\alpha)\lambda_2^{-1}+\alpha\right)\lambda_2^{1-q}\left(1-\beta+\beta\kappa_1\right)\kappa_1^p, \tag{14}$$

is non-zero. We denote the factors in equation (14) as

$$\begin{aligned} a_1 &:= (1-\alpha)\lambda_2^{-1}+\alpha, \\ a_2 &:= \lambda_2^{1-q}, \\ a_3 &:= 1-\beta+\beta\kappa_1, \\ a_4 &:= \kappa_1^p. \end{aligned}$$

The determinant is zero if the product $a_1a_2a_3a_4$ equals one. A necessary condition for $\Delta = 0$ is therefore

$$|a_1||a_2||a_3||a_4| = 1. \tag{15}$$

Note that $|a_2| = |\lambda_2|^{1-q} \leq 1$ if $q \geq 1$ and $|a_4| = |\kappa_1|^p \leq 1$ if $p \geq 0$. Furthermore,

$$|a_1|^2 = (1-\alpha)^2|\lambda_2^{-1}|^2+\alpha^2+2\alpha(1-\alpha)\mathrm{Re}(\lambda_2^{-1}), \tag{16}$$

$$|a_3|^2 = (1-\beta)^2+\beta^2|\kappa_1|^2+2\beta(1-\beta)\mathrm{Re}(\kappa_1). \tag{17}$$

Since $\mathrm{Re}(\lambda_2^{-1})-|\lambda_2^{-1}| \leq 0$, we have

$$\begin{aligned} |a_1|^2 &= \left((1-\alpha)|\lambda_2^{-1}|+\alpha\right)^2+2\alpha(1-\alpha)\left(\mathrm{Re}(\lambda_2^{-1})-|\lambda_2^{-1}|\right) \\ &\leq \left((1-\alpha)|\lambda_2^{-1}|+\alpha\right)^2 \leq \max\left(|\lambda_2^{-1}|^2,1\right) \leq 1, \quad 0 \leq \alpha < 1. \end{aligned}$$

The same argument applies to $|a_3|$ and we have $|a_3| \leq \max(|\kappa_1|,1) \leq 1$ for $0 \leq \beta < 1$. Because all factors $|a_i|$ in (15) are less than or equal to one, their product can only be one if all the factors are equal to one. But, if $q \geq 2$ and $p \geq 1$, $|a_2| = |a_4| = 1$ implies

$$|\kappa_1| = 1, \quad |\lambda_2| = 1. \tag{18}$$

From lemma 4 we have that $|\kappa_1(h_1s)| = |\lambda_2(h_2s)| = 1$ for $s \in I$, where the interval I is defined by

$$I := \left\{ s = i\xi, \ -\min\left(\frac{1}{h_1},\frac{1}{h_2}\right) \leq \xi \leq \min\left(\frac{1}{h_1},\frac{1}{h_2}\right)\right\}. \tag{19}$$

Therefore, the determinant (14) is non-zero in the right half-plane $\mathrm{Re}(s) \geq 0$, outside the interval I. We next study the determinant in the part of the imaginary axis $\mathrm{Re}(s) = 0$ where $s \in I$. Inserting (18) into (16) and (17) give

$$\begin{aligned} |a_1|^2 &= (\alpha^2-\alpha)\left(2-2\mathrm{Re}(\lambda_2^{-1})\right)+1, \\ |a_3|^2 &= (\beta^2-\beta)\left(2-2\mathrm{Re}(\kappa_1)\right)+1. \end{aligned}$$

From lemma 4, we have $0 \le \mathrm{Re}(\lambda_2^{-1}) \le 1$, and $\mathrm{Re}(\lambda_2^{-1}) = 1$ at $s = 0$. Hence, for $s \in I$, the function $|a_1|$ satisfies

$$|a_1| \begin{cases} = 1, & s = 0, \quad\quad\quad\quad 0 \le \alpha < 1, \\ = 1, & s \in I, \quad\quad\quad\quad \alpha = 0, \\ < 1, & s \in I, \quad s \ne 0, \quad 0 < \alpha < 1. \end{cases} \tag{20}$$

The behavior of the term $|a_3|$ is simpler because $2 - 2\mathrm{Re}(\kappa_1) \ge 2$ for $\mathrm{Re}(s) \ge 0$. Therefore $|a_3| < 1$ for $0 < \beta < 1$ and $|a_3| = 1$ at $\beta = 0$. Note that we have so far only investigated $P := |a_1||a_2||a_3||a_4|$, and that $P = 1$ is a necessary, but not a sufficient condition for $\Delta = 0$. We conclude that $P < 1$, which implies that the determinant (14) is non-zero, for $s \in I$ if $\beta \ne 0$.

We proceed by investigating the case when $\beta = 0$ for $s \in I$. Because $|\kappa_1(h_1 i\xi)| = 1$ and $|\lambda_2(h_2 i\xi)| = 1$ we have

$$\begin{aligned} \kappa_1(h_1 i\xi) &= ih_1\xi - \sqrt{1 - (h_1\xi)^2} =: e^{i\theta_1}, \\ \lambda_2(h_2 i\xi) &= ih_2\xi + \sqrt{1 - (h_2\xi)^2} =: e^{i\theta_2}. \end{aligned}$$

In the case $\beta = 0$, the determinant (14) simplifies to

$$\Delta = 1 - \left((1 - \alpha)e^{-i\theta_2} + \alpha\right) e^{i(1-q)\theta_2} e^{ip\theta_1}.$$

If $\alpha \ne 0$, we know from (20) that only the case $s = 0$ must be considered. We then have $\theta_1 = \pi$ and $\theta_2 = 0$. Therefore,

$$\Delta = 1 - e^{ip\pi} = 1 - (-1)^p = 0, \quad p = 2, 4, 6, \ldots. \tag{21}$$

Because $\theta_2 = 0$, (21) is satisfied for all $0 \le \alpha < 1$.

If $\alpha = 0$ and $\beta = 0$, we must investigate if there are any additional eigenvalues in the interval (19) except $s = 0$. In this case, the overlap relations yield

$$qh_2 = ph_1, \quad q \ge 2, \quad p \ge 1. \tag{22}$$

In the trivial case when $h_1 = h_2$, the original problem (5), (6) reduces to a one-grid problem for which an energy estimate easily can be derived. We can therefore focus on the case $h_1 \ne h_2$. The determinant (14) now satisfies

$$\Delta = 1 - e^{i(p\theta_1 - q\theta_2)}. \tag{23}$$

It is easy to see that solutions of $\Delta = 0$ come in complex conjugated pairs: $s = \pm i\xi$. It therefore suffices to consider $0 < \xi \le \min(1/h_1, 1/h_2)$ where the angles θ_1 and θ_2 satisfy $\pi/2 < \theta_1 \le \pi$ and $0 < \theta_2 \le \pi/2$. We therefore have

$$\begin{aligned} \theta_1(\xi) &= \pi - \arctan\left(\frac{h_1\xi}{\sqrt{1 - (h_1\xi)^2}}\right), \\ \theta_2(\xi) &= \arctan\left(\frac{h_2\xi}{\sqrt{1 - (h_2\xi)^2}}\right). \end{aligned}$$

The determinant (23) is zero if $p\theta_1 - q\theta_2 = 2k\pi$ for some $k = 0, \pm 1, \pm 2, \ldots$. This is equivalent to

$$p \arctan\left(\frac{h_1\xi}{\sqrt{1-(h_1\xi)^2}}\right) + q \arctan\left(\frac{h_2\xi}{\sqrt{1-(h_2\xi)^2}}\right) = \pi(p-2k). \tag{24}$$

We set

$$r = \frac{h_2}{h_1} = \frac{p}{q}, \quad \tilde{\xi}_1 = h_1\xi, \quad \tilde{\xi}_2 = h_2\xi.$$

Equation (24) can be written as

$$\arctan\left(\frac{\tilde{\xi}_1}{\sqrt{1-\tilde{\xi}_1^2}}\right) + \frac{1}{r}\arctan\left(\frac{r\tilde{\xi}_1}{\sqrt{1-(r\tilde{\xi}_1)^2}}\right) = \pi\left(\frac{p-2k}{p}\right), \tag{25}$$

or equivalently

$$\arctan\left(\frac{\tilde{\xi}_2}{\sqrt{1-\tilde{\xi}_2^2}}\right) + \frac{1}{r^{-1}}\arctan\left(\frac{r^{-1}\tilde{\xi}_2}{\sqrt{1-(r^{-1}\tilde{\xi}_2)^2}}\right) = \pi r\left(\frac{p-2k}{p}\right). \tag{26}$$

We will use (25) when $r < 1$ and (26) when $r > 1$. The intervals we must consider are therefore $0 < \tilde{\xi}_1 \leq 1$ and $0 < \tilde{\xi}_2 \leq 1$, respectively. Elementary properties of the function $\arctan(x)$ yield

$$0 < \arctan\left(\frac{\tilde{\xi}}{\sqrt{1-\tilde{\xi}^2}}\right) + \frac{1}{r}\arctan\left(\frac{r\tilde{\xi}}{\sqrt{1-(r\tilde{\xi})^2}}\right) < \frac{\pi}{2} + \frac{1}{r}\arctan\left(\frac{r}{\sqrt{1-r^2}}\right),$$

for $0 < \tilde{\xi} \leq 1$, $0 < r < 1$. We also have that

$$1 < \frac{1}{r}\arctan\left(\frac{r}{\sqrt{1-r^2}}\right) < \frac{\pi}{2}, \quad 0 < r < 1.$$

When $r < 1$ there is therefore a solution of (25) for every integer k such that

$$0 < \pi\left(\frac{p-2k}{p}\right) < \frac{\pi}{2} + \frac{1}{r}\arctan\left(\frac{r}{\sqrt{1-r^2}}\right) < \pi.$$

These solutions exist for $p \geq 3$. For example, the case $p = 3$ and $q = 4$ is solved by $\tilde{\xi}_1 \approx 0.1661$ with $k = 1$. Similarly, when $r > 1$, (26) has a solution for every integer k such that

$$0 < \pi r\left(\frac{p-2k}{p}\right) < \frac{\pi}{2} + \frac{1}{r^{-1}}\arctan\left(\frac{r^{-1}}{\sqrt{1-r^{-2}}}\right) < \pi.$$

Also these solutions exist for $p \geq 3$. One example is $p = 3$ and $q = 2$, where $\tilde{\xi}_2 \approx 0.7262$ and $k = 1$ is a solution of (26).

We summarize the analysis of the determinant (14) in the half-plane $\mathrm{Re}(s) \geq 0$ in Lemma 5.

Lemma 5 *The determinant (14) is non-zero in the half-plane $Re(s) \geq 0$, for $s \notin I$. If $\beta \neq 0$, the determinant is also non-zero for $s \in I$. If $\beta = 0$ the determinant is zero at $s = 0$ if $p = 2, 4, 6, \ldots$. If also $\alpha = 0$, the case $p/q = 1$ is ignored because it corresponds to discretizing the original problem on one grid where the stability can be shown by an energy estimate. However, if $p/q \neq 1$, there are additional zeros to the determinant if $p \geq 3$; we will denote these roots $s = \pm i\xi_k$. When $p/q < 1$ they are the solutions of (25) and when $p/q > 1$ they follow as the solutions of (26). Thus,*

$$\Delta(s) \begin{cases} \neq 0, & Re(s) \geq 0, \ s \notin I, \\ \neq 0, & s \in I \ \cap \ \beta \neq 0, \\ = 0, & s = 0 \ \cap \ \beta = 0 \ \cap \ p = 2, 4, 6, \ldots, \\ = 0, & s = \pm i\xi_k \ \cap \ \alpha = \beta = 0 \ \cap \ p \neq q \ \cap \ p \geq 3. \end{cases}$$

Applying Lemma 5 to the system (13) reveals when there are eigenvalues or generalized eigenvalues of (9) (and equivalently (8)). Because the zero's of $\Delta(s)$ have $\mathrm{Re}(s) = 0$ and correspond to $|\kappa| = 1$, they are generalized eigenvalues. This proves Lemma 3.

The eigenfunction corresponding to $s = 0$, $\beta = 0$ and p even is

$$\hat{y}_j^{(1)} = \sigma_1(-1)^j, \quad \hat{y}_j^{(2)} \equiv \tau_2. \tag{27}$$

We note in passing that the characteristic of (1) is $x(t) = x_0 - t$, i.e. the solution of (1) is a translation of the initial data to the left with velocity one. Hence, the eigenfunction (27) is constant to the left (downstream) of the overlap region, and oscillates rapidly to the right (upstream) of the overlap region.

Because the L_2-norm of (27) is unbounded, we call $s = 0$ a generalized eigenvalue. To determine the stability properties of $s = 0$ when $\beta = 0$ we expand Δ around $s = 0$. The factors in (14) satisfy

$$\begin{aligned} \kappa_1(h_1 s) &= -1 + h_1 s + \mathcal{O}((h_1 s)^2), \\ \lambda_2(h_2 s) &= 1 + h_2 s + \mathcal{O}((h_2 s)^2), \end{aligned}$$

and by the standard formula for binomial series,

$$\begin{aligned} \kappa_1^p(h_1 s) &= (-1)^p + p(-1)^{p-1} h_1 s + \mathcal{O}((h_1 s)^2), \\ \lambda_2^{-q}(h_2 s) &= 1 - q h_2 s + \mathcal{O}((h_2 s)^2). \end{aligned}$$

For even p we therefore have

$$\Delta(s) = 1 - (1 - \alpha + \alpha\lambda_2)\lambda_2^{-q}\kappa_1^p = (p h_1 + (q - \alpha) h_2) s + \mathcal{O}(s^2).$$

Because $\beta = 0$, the overlapping relation is

$$(q - \alpha) h_2 = p h_1,$$

and we see that the factor in front of the s-term equals twice the size of the overlap region, which by definition always is positive. Hence, the generalized eigenvalue $s = 0$ corresponds to a simple zero of the determinant Δ. By the theory in [5], section 12.5, we have that this type of eigenvalue makes the corresponding strip problem severely unstable, i.e. the instability grows with mesh refinement. In absolute terms, however, our computational examples show that the instability is still moderate, see section 5.

By the same arguments, the eigenvalues in the interval I on the imaginary axis in the case $\alpha = \beta = 0$ and $p \geq 3$ are also simple roots of the determinant and since $|\kappa_1| = |\lambda_2| = 1$ these are also generalized eigenvalues of the bad type.

4 The Viscous Interpolation Problem

In this section we perform the same analysis as in the previous section but for the viscous wave equation:

$$\begin{aligned} u_t &= u_x + \nu u_{xx}, \quad t \geq 0, \quad -\infty < x < \infty, \\ u(0,x) &= f(x), \qquad \int_{-\infty}^{\infty} |f(x)|^2 \, dx < \infty. \end{aligned} \tag{28}$$

By discretizing the viscous term with second order centered differences and forming the eigenvalue problem corresponding to (9), we get

$$\begin{aligned} 2sh_1\hat{y}_j^{(1)} &= \hat{y}_{j+1}^{(1)} - \hat{y}_{j-1}^{(1)} + 2\epsilon_1(\hat{y}_{j+1}^{(1)} - 2\hat{y}_j^{(1)} + \hat{y}_{j-1}^{(1)}), \quad j = 1, 2, \ldots, \\ 2sh_2\hat{y}_j^{(2)} &= \hat{y}_{j+1}^{(2)} - \hat{y}_{j-1}^{(2)} + 2\epsilon_2(\hat{y}_{j+1}^{(2)} - 2\hat{y}_j^{(2)} + \hat{y}_{j-1}^{(2)}), \quad j = q-1, q-2, \ldots, \\ \hat{y}_0^{(1)} &= (1-\alpha)\hat{y}_0^{(2)} + \alpha\hat{y}_1^{(2)}, \\ \hat{y}_q^{(2)} &= (1-\beta)\hat{y}_p^{(1)} + \beta\hat{y}_{p+1}^{(1)}, \end{aligned} \tag{29}$$

where $\epsilon_k = \nu/h_k > 0$, $k = 1, 2$. We will prove

Lemma 6 *Let $p \geq 1$ and $q \geq 2$. For positive viscosities, $\nu > 0$, there are no eigenvalues or generalized eigenvalues of the system (29) in $Re(s) \geq 0$.*

As in the inviscid case, the general solution to the system (29) is

$$\begin{aligned} \hat{y}_j^{(1)} &= \sigma_1\kappa_1^j + \sigma_2\kappa_2^j, \qquad j = 0, 1, \ldots, \\ \hat{y}_j^{(2)} &= \tau_1\lambda_1^{j-q} + \tau_2\lambda_2^{j-q}, \quad j = q, q-1, \ldots, \end{aligned} \tag{30}$$

where κ_k, λ_k are the roots of the characteristic equations obtained by inserting (30) into the difference approximation (29), i.e.

$$\begin{aligned} 2\tilde{s}_1\kappa &= \kappa^2 - 1 + 2\epsilon_1(\kappa^2 - 2\kappa + 1), \qquad \tilde{s}_1 = h_1 s, \\ 2\tilde{s}_2\lambda &= \lambda^2 - 1 + 2\epsilon_2(\lambda^2 - 2\lambda + 1), \qquad \tilde{s}_2 = h_2 s. \end{aligned} \tag{31}$$

Thus,

$$\begin{aligned}\kappa_{1,2}(\tilde{s}_1) &= \frac{1}{1+2\epsilon_1}\left(\tilde{s}_1 + 2\epsilon_1 \mp \sqrt{1+\tilde{s}_1^2+4\epsilon_1\tilde{s}}\right), \\ \lambda_{1,2}(\tilde{s}_2) &= \frac{1}{1+2\epsilon_2}\left(\tilde{s}_2 + 2\epsilon_2 \mp \sqrt{1+\tilde{s}_2^2+4\epsilon_2\tilde{s}}\right).\end{aligned} \tag{32}$$

As in the inviscid case, the solution is bounded if $\sigma_2 = \tau_1 = 0$, because $|\kappa_2| \geq 1$ and $|\lambda_1| < 1$ for $\mathrm{Re}(s) \geq 0$. Similar to the inviscid case, $|\lambda_2| \geq 1$ for $\mathrm{Re}(s) \geq 0$. The important difference obtained by adding viscosity is that $|\kappa_1| < 1$ for $\mathrm{Re}(s) \geq 0$. Using the notation of Lemma 4, the properties of λ_1 and κ_2 are stated in Lemma 7 and illustrated in figure 3.

Lemma 7 *Consider the functions*

$$\begin{aligned}\kappa_1(\tilde{s}) &= \frac{1}{1+2\epsilon_1}\left(\tilde{s} + 2\epsilon_1 - \sqrt{1+\tilde{s}^2+4\epsilon_1\tilde{s}}\right), \\ \lambda_2(\tilde{s}) &= \frac{1}{1+2\epsilon_2}\left(\tilde{s} + 2\epsilon_2 + \sqrt{1+\tilde{s}^2+4\epsilon_2\tilde{s}}\right),\end{aligned}$$

where $\epsilon_k > 0$, $k = 1, 2$, *and*

$$-\frac{\pi}{2} \leq \arg\sqrt{1+\tilde{s}^2+4\epsilon_k\tilde{s}} \leq \frac{\pi}{2}, \qquad \textit{for} \qquad Re(s) \geq 0.$$

The function $\kappa_1(\tilde{s})$, maps the complex half-plane $Re(\tilde{s}) \geq 0$ to a sub-domain of the interior of the left half of the unit disc, $\kappa_1 \subset\subset D_l$ for $Re(\tilde{s}) \geq 0$. In particular, $|\kappa_1(\tilde{s})| < 1$. The function $\lambda_2(\tilde{s})$ maps $Re(\tilde{s}) \geq 0$ to a sub-domain of the exterior of the right half of the unit disc, $\lambda_2 \subset \bar{D}_r$. However, $\lambda_2(0) = 1$, so $|\lambda_2| \geq 1$ for $Re(\tilde{s}) \geq 0$.

The definition (14) of the determinant Δ is the same as in the inviscid case and therefore, because $|\kappa_1| < 1$,

$$\Delta \neq 0, \qquad \mathrm{Re}(s) \geq 0, \qquad \nu > 0.$$

Thus, there are no non–trivial solutions of (29) in $\mathrm{Re}(s) \geq 0$. This proves Lemma 6.

5 The Strip Problem

In this section we will investigate the inviscid wave equation (1) and its viscous counterpart (28) for the strip problem $x \in \Omega_2$. After an eigenvalue analysis similar to that in previous sections we numerically compute the solutions of the inviscid and viscous wave equations.

As we have noted before, the solution of (1) is $u(t,x) = f(x-t)$, i.e. a wave moving with speed 1 to the left. We therefore prescribe a Dirichlet boundary condition at $x = 2\pi$: $u_m^{(1)} = h(t)$, where the characteristic is in-going. At $x = 0$, where the characteristic is outgoing, we must give a numerical condition for the discretized system. Here, the solution is extrapolated linearly to the boundary point $u_{-n}^{(2)}$. The indexing of the grid points is shown in figure 4.

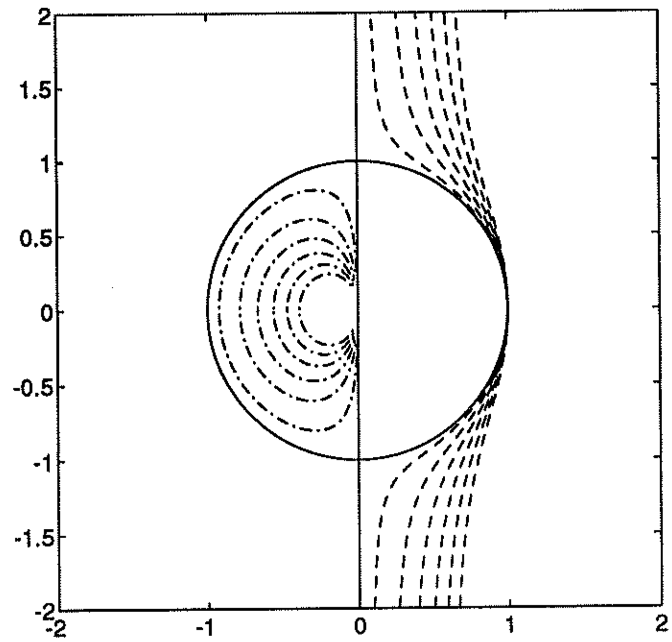

Figure 3: Mappings of the imaginary axis by the functions $\kappa_1(i\xi)$ (dash–dotted) and $\lambda_2(i\xi)$ (dashed), $-1.6 \leq \xi \leq 1.6$ for different values of $\epsilon_{1,2}$ in the interval $0.02 \leq \epsilon_{1,2} \leq 0.2$. The inviscid case $\epsilon_{1,2} = 0$ is described in figure 2.

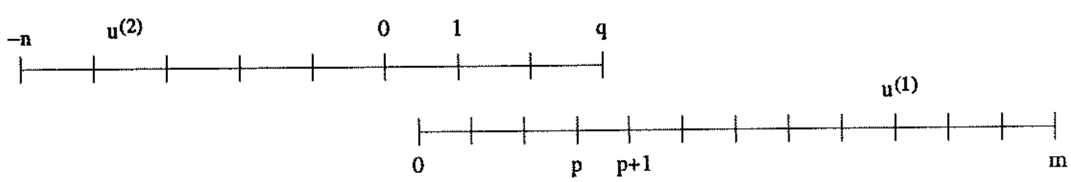

Figure 4: Schematic picture of overlapping grids for the strip problem.

The semi-discrete strip problem is

$$
\begin{aligned}
\frac{\partial u_j^{(1)}}{\partial t} &= \frac{u_{j+1}^{(1)} - u_{j-1}^{(1)}}{2h_1}, && j = 1, 2, \ldots, m-1, \\
\frac{\partial u_j^{(2)}}{\partial t} &= \frac{u_{j+1}^{(2)} - u_{j-1}^{(2)}}{2h_2}, && j = q-1, \ldots, -n+1, \\
u_m^{(1)} &= h(t), \\
u_0^{(1)} &= (1-\alpha)u_0^{(2)} + \alpha u_1^{(2)}, \\
u_q^{(2)} &= (1-\beta)u_p^{(1)} + \beta u_{p+1}^{(1)}, \\
u_{-n}^{(2)} &= 2u_{-n+1}^{(2)} - u_{-n+2}^{(2)}, \\
u_j^{(k)}(0) &= f_j^{(k)}, \quad k = 1, 2,
\end{aligned}
\tag{33}
$$

As was discussed in the introduction, the strip problem can be seen as an initial boundary value problem for the vector variable $(u_j^{(1)}, u_j^{(2)})^T$. At one boundary we have the interpolation relations and at the other boundary we have in/outflow boundary conditions. By using the theory of section 2, we know that the strip problem is stable if both the left and right half-plane problems are stable. It is not difficult to show that the half-plane problem with the in/outflow boundary conditions is stable and that the remaining conditions of Theorem 1 are satisfied. We therefore know that the stability of the strip problem is determined by the stability of the interpolation problem. Our stability definition allows for exponential growth, and we will in the present section investigate how the growth rate depends on the overlap parameters.

The eigenvalue problem corresponding to (33) is

$$
\begin{aligned}
2h_1 s\hat{y}_j^{(1)} &= \hat{y}_{j+1}^{(1)} - \hat{y}_{j-1}^{(1)}, && j = 1, 2, \ldots, m-1, \\
2h_2 s\hat{y}_j^{(2)} &= \hat{y}_{j+1}^{(2)} - \hat{y}_{j-1}^{(2)}, && j = q-1, \ldots, -n+1, \\
\hat{y}_m^{(1)} &= 0 \\
\hat{y}_0^{(1)} &= (1-\alpha)\hat{y}_0^{(2)} + \alpha\hat{y}_1^{(2)}, \\
\hat{y}_q^{(2)} &= (1-\beta)\hat{y}_p^{(1)} + \beta\hat{y}_{p+1}^{(1)}, \\
\hat{y}_{-n}^{(2)} &= 2\hat{y}_{-n+1}^{(2)} - \hat{y}_{-n+2}^{(2)}.
\end{aligned}
\tag{34}
$$

Using the Ansatz

$$
\begin{aligned}
\hat{y}_j^{(1)} &= \sigma_1\kappa_1^j + \sigma_2\kappa_2^j, && j = 0, 1, \ldots, m, \\
\hat{y}_j^{(2)} &= \tau_1\lambda_1^j + \tau_2\lambda_2^j, && j = q, q-1, \ldots, -n,
\end{aligned}
\tag{35}
$$

we get the same characteristic equations for κ_k and λ_k as in the interpolation problem (12). The boundary and interpolation conditions give the following system of equations for τ_k and σ_k, $k = 1, 2$:

$$\begin{pmatrix} \kappa_1^m & \kappa_2^m & 0 & 0 \\ 1 & 1 & \alpha-\alpha\lambda_1-1 & \alpha-\alpha\lambda_2-1 \\ (\beta-\beta\kappa_1-1)\kappa_1^p & (\beta-\beta\kappa_2-1)\kappa_2^p & \lambda_1^q & \lambda_2^q \\ 0 & 0 & (1-2\lambda_1+\lambda_1^2)\lambda_1^{2-n} & (1-2\lambda_2+\lambda_2^2)\lambda_2^{2-n} \end{pmatrix} \begin{pmatrix} \sigma_1 \\ \sigma_2 \\ \tau_1 \\ \tau_2 \end{pmatrix} = 0. \tag{36}$$

An eigenvalue s of (34) is thus a root of the equation

$$\det(a_{ij}) = 0, \tag{37}$$

where (a_{ij}), $i, j = 1, \ldots, 4$ is the coefficient matrix in (36). (This equation corresponds to equation (14) for the interpolation problem.) For some values of the grid parameters α, β, h_k, p, q etc., there are roots s to (37) with $\mathrm{Re}(s) > 0$ and thus the semi-discrete problem has exponentially fast growing modes for these grids. We will calculate such roots numerically for a few test grids given below, where we will denote by s_l the root with the largest real part. The expected growth

$$\|u^{(i)}\|_{h_k} \sim e^{\delta t}, \quad \delta = \mathrm{Re}(s_l) \tag{38}$$

compares accurately with the growth in the numerical solution of (33).

We will take the initial and boundary data to be

$$f(x) = \sin(x), \tag{39}$$

$$h(t) = \sin(at), \quad a = \frac{\sin(h_1)}{h_1}. \tag{40}$$

The factor $\sin(h_1)/h_1$ is included to correct the boundary data for the numerical phase error on grid 1 so the value at the inflow corresponds better to the wave propagation speed on grid 1. The numerical solution is calculated with a fourth order (classical) Runge-Kutta method in time. The time step is chosen at least ten times smaller than required by the stability limits of the Runge-Kutta method as to avoid the dissipation which otherwise could damp out an expected growth. (That a growing mode in some cases can be neutralized by discretizing time with a fourth order Runge-Kutta method reveals how weak the growing mode is for this system.) For all grids, we take $x_m^{(1)} = 2\pi$ and $x_{-n}^{(2)} = 0$. The overlap parameters are uniquely determined if, say, $h_2/h_1, \alpha$, and q are given. The numbers m and n determine the location of the overlap, denoted in the tables below by $x_0^{(1)}$, which is the coordinate of the first grid point in mesh 1.

We first focus on the "bad" overlaps, i.e. the overlaps for which there are generalized eigenvalues for the inviscid interpolation problem. Such eigenvalues can in general not be accepted for the strip problem, as is shown by Gustafsson et al. [5], because a disturbance is not damped away from the interpolation boundary and it can be amplified and reflected at the in/outflow boundary.

Overlap parameters				
h_1/h_2	α	(β)	(p)	q
2.1	0.1429	0.	6	3

Grid parameters			eigenvalue	growth
m	n	$(x_0^{(1)})$	s_l	δ
16	8	3.23	4.489e-02 + i2.346e+00	4.142e-02
32	16	3.23	7.249e-02 + i4.379e+00	7.190e-02
64	32	3.23	1.018e-01 + i9.253e+00	1.016e-01
128	64	3.23	1.851e-01 + i1.889e+01	1.844e-01
256	128	3.23	2.094e-01 + i3.699e+01	2.095e-01
512	256	3.23	2.575e-01 + i7.456e+01	2.567e-01

Table 1: Grid parameters for a "bad" overlap. The growth rate δ increases with mesh refinement.

In table 1 are listed the grid parameters and the growth rate of the solution when the system (33) is solved on overlapping grids with a "bad" overlap of the first type, i.e. $\beta = 0$ and $p \geq 2$ is even. We note that the growth rate δ increases with mesh refinement. Figure 5 shows δ as a function of m, on a logarithmic scale, where m is the number of grid points in mesh 1. If a straight line is fitted to these data we find that the growth is of the order

$$e^{\delta t} \sim m^{\gamma t}, \quad \gamma \approx 0.065. \tag{41}$$

The situation is similar for the second kind of "bad" overlap when $\alpha = \beta = 0,\ p \geq 3$ is odd. Table 2 gives the grid parameters and the growth rate. Figure 6 shows how the growth rate increases with mesh refinement and here

$$e^{\delta t} \sim m^{\gamma t}, \quad \gamma \approx 0.033. \tag{42}$$

For comparison we have in Table 3 included a case with a "good" overlap, i.e. a overlap which has no eigenvalues in $\mathrm{Re}(s) \geq 0$ for the interpolation problem. First we note that the growth rate is smaller than for "bad" overlaps studied earlier and also that the growth rate decreases with mesh refinement. However, for most overlaps in this category the solution will show no growth at all.

One remedy to the problem of having growing modes is to add some dissipation, which will remove the generalized eigenvalues for the interpolation problem, as was shown in section 4. The question is how much viscosity is needed to cancel the growth and if this

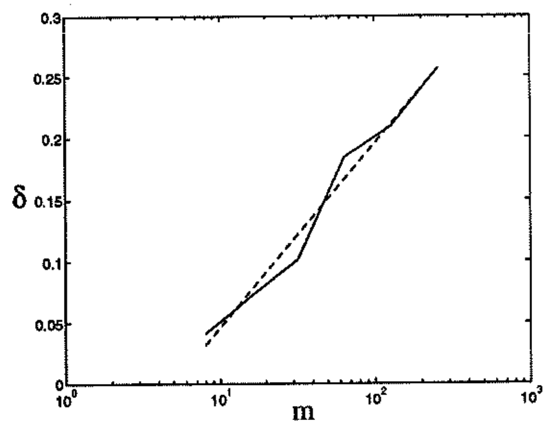

Figure 5: The growth rate δ as a function of the number of grid points m for the grid of Table 1. The dashed line shows a least square fit of the function $A + \gamma \log(m)$, which gave $\gamma = 0.065$.

Overlap parameters				
h_1/h_2	α	(β)	(p)	q
0.5	0.	0.	5	10

Grid parameters			eigenvalue	growth
m	n	$(x_0^{(1)})$	s_l	δ
32	8	0.70	5.833e-02 + i4.945e+00	5.831e-02
64	16	0.70	1.029e-01 + i9.732e+00	1.029e-01
128	32	0.70	1.094e-01 + i1.930e+01	1.104e-01
256	64	0.70	1.345e-01 + i3.898e+01	1.348e-01
512	128	0.70	1.556e-01 + i7.823e+01	1.556e-01

Table 2: Grid parameters for a "bad" overlap. The growth rate δ increases with mesh refinement.

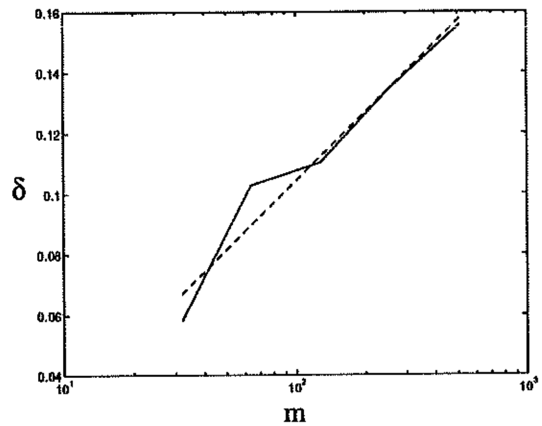

Figure 6: The growth rate δ as a function of the grid refinement m for the grid of Table 2. The dashed line shows a least square fit of the function $A + \gamma \log(m)$, which gave $\gamma = 0.033$.

Overlap parameters				
h_1/h_2	α	(β)	(p)	q
1.7	0.3	0.59	4	3

Grid parameters			eigenvalue	growth
m	n	$(x_0^{(1)})$	s_l	δ
16	32	4.87	1.040e-02 + i6.473e+00	1.026e-02
32	64	4.87	8.377e-03 + i1.275e+01	8.507e-03
64	128	4.87	5.371e-03 + i2.512e+01	5.635e-03

Table 3: Grid parameters for a "good" overlap. The growth rate δ decreases with mesh refinement.

Overlap parameters				
h_1/h_2	α	(β)	(p)	q
2.1	0.1429	0.	6	3

Grid parameters				eigenvalue	growth
m	n	$(x_0^{(1)})$	ν_2	s_l	δ
32	16	3.23	0.000e+00	7.249e-02 + i4.379e+00	7.190e-02
32	16	3.23	1.000e-04	6.213e-02 + i4.380e+00	6.168e-02
32	16	3.23	2.000e-04	5.200e-02 + i4.382e+00	5.149e-02
32	16	3.23	4.000e-04	3.243e-02 + i4.383e+00	3.295e-02
32	16	3.23	6.000e-04	1.371e-02 + i4.383e+00	1.321e-02
32	16	3.23	7.390e-04	1.173e-03 + i4.383e+00	0.000e+00
64	32	3.23	0.000e+00	1.018e-01 + i9.253e+00	1.016e-01
64	32	3.23	1.000e-04	7.047e-02 + i9.282e+00	7.012e-02
64	32	3.23	2.000e-04	3.897e-02 + i9.297e+00	3.946e-02
64	32	3.23	3.000e-04	8.640e-03 + i9.305e+00	9.432e-03
64	32	3.23	3.280e-04	4.000e-04 + i9.307e+00	0.000e+00

Table 4: Grid parameters for a "bad" overlap. The solution of the wave equation is computed with second order artificial viscosity $\nu_2 D_+ D_- u_j$. The growth rate δ decreases with increasing viscosity.

will affect the accuracy of the solution. In Table 4 are listed the results from solving the system (33) with the dissipation terms $\nu_2 D_+ D_- u_j^{(k)}$, $k = 1,2$, added to the first and second equations, respectively. First we consider the grids from Table 1. Figure 7 shows the decrease of the growth rate as function of increasing viscosity ν_2. Although the viscosity needed to completely remove the growth is small, we note that it only decreases by a factor 2 when the number of grid points is doubled. Thus the amount of viscosity required for a "bad" overlap is of the order

$$\nu_2 \sim O(h),$$

and the method is only first order accurate with respect to the inviscid wave equation (1).

We next investigate how the same dissipation terms change the growth rate of the solution when the grid from Table 3 is used, where the overlap is of the "good" type. The

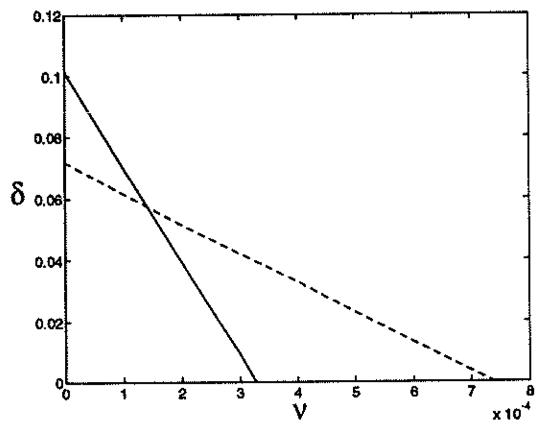

Figure 7: The growth rate δ as a function of the coefficient of the second order viscosity, ν_2, for a "bad" overlap with two grid refinements. The dashed line is computed with $m = 32$ and the solid line with $m = 64$. Note that the amount of viscosity only decreases by a factor two when the number of grid points is doubled.

results are given in Table 5 and Figure 8. Here we need less viscosity since the growth rate is smaller. Furthermore, the amount of viscosity needed to cancel the growth decreases by a factor 4 when the number of grid points is doubled. Thus, for a "good" overlap the amount of viscosity is

$$\nu_2 \sim O(h^2).$$

Therefore, the method remains second order accurate with respect to the inviscid equation (1), despite the addition of the artificial dissipation term.

We end this section by reporting how a fourth order artificial dissipation term affects the solution of the wave equation. In this case, an analysis is more difficult, and we will only report on the results of our numerical experiments. We solved the system (33) with the additional terms $-\nu_4 D_-^2 D_+^2 u_j^{(k)}$, $k = 1, 2$, added to the first and second equations, respectively. The results are given in Table 6 and Figure 9. By decreasing the grid size, we found that for the grids that previously gave the worst growth (Table 1 and 4), the minimum amount of viscosity to cancel the spurious growth is

$$\nu_4 \sim O(h^3),$$

or possibly less. We therefore conclude that the method remains second order accurate for all types of overlaps.

Overlap parameters				
h_1/h_2	α	(β)	(p)	q
1.7	0.3	0.59	4	3

Grid parameters				eigenvalue	growth
m	n	$(x_0^{(1)})$	ν_2	s_l	δ
16	32	4.87	0.000e+00	1.040e-02 + i6.473e+00	1.026e-02
16	32	4.87	1.000e-05	9.172e-03 + i6.473e+00	1.013e-02
16	32	4.87	4.000e-05	5.521e-03 + i6.473e+00	6.000e-03
16	32	4.87	8.000e-05	6.824e-04 + i6.473e+00	none
32	64	4.87	0.000e+00	8.377e-03 + i1.275e+01	8.507e-03
32	64	4.87	1.000e-05	3.923e-03 + i1.275e+01	4.357e-03
32	64	4.87	1.800e-05	3.705e-04 + i1.275e+01	none

Table 5: Grid parameters for a "good" overlap. The solution of the wave equation is computed with second order artificial viscosity $\nu_2 D_+ D_- u_j$. The growth rate δ decreases with increasing viscosity.

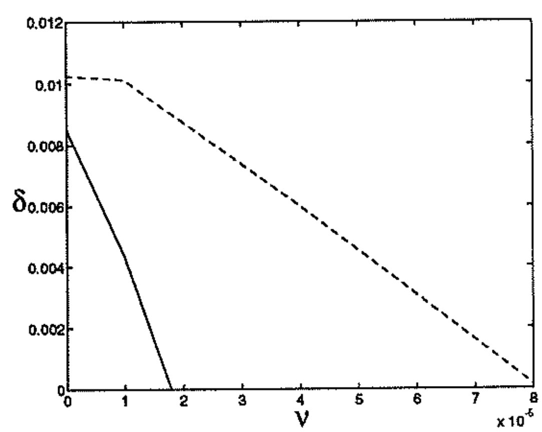

Figure 8: The growth rate δ as a function of the viscosity ν_2 for a "good" overlap with two grid refinements. The dashed line is computed with $m = 16$ and the solid line with $m = 32$. Note that the amount of viscosity decreases by a factor four when the number of grid points is doubled.

Overlap parameters				
h_1/h_2	α	(β)	(p)	q
2.1	0.1429	0.	6	3

Grid parameters				growth
m	n	$(x_0^{(1)})$	ν_4	δ
32	16	3.225	0.000e+00	7.190e-02
32	16	3.225	1.000e-06	5.012e-03
32	16	3.225	2.000e-06	2.820e-03
32	16	3.225	3.000e-06	1.626e-03
32	16	3.225	4.000e-06	1.156e-03
32	16	3.225	5.000e-06	6.016e-04
32	16	3.225	6.000e-06	none
64	32	3.225	0.000e+00	1.016e-01
64	32	3.225	2.000e-07	2.681e-04
64	32	3.225	5.000e-07	7.234e-04
64	32	3.225	6.250e-07	none

Table 6: Grid parameters for a "bad" overlap. The solution of the wave equation is computed with a fourth order artificial viscosity $-\nu_4 D_+^2 D_-^2 u_j$. The growth rate δ decreases with increasing viscosity. Note the dramatic decrease in the growth rate when the viscosity $\nu_4 = 10^{-6}$ is introduced for the coarser grid and, likewise, when $\nu_4 = 2 \cdot 10^{-7}$ is applied to the finer mesh.

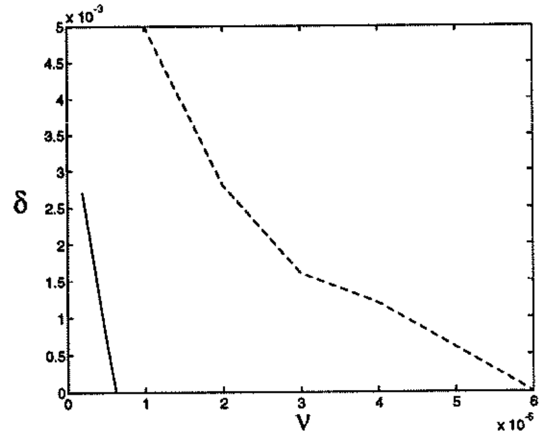

Figure 9: The growth rate δ as a function of the coefficient of the fourth order viscosity, ν_4, for a "bad" overlap with two grid refinements. The dashed line is computed with $m = 32$ and the solid line with $m = 64$. Here, $\nu_4 \sim O(h^3)$ is sufficient to cancel the spurious growth, and thus the artificial viscosity will not affect the overall accuracy of the method.

6 Discussion

From the analysis and the numerical experiments presented above it is clear that when a one-dimensional hyperbolic problem is solved with finite differences on an overlapping grid, some dissipation must be introduced to remove possible spuriously growing modes. We have demonstrated that for most overlap parameters, the solution will not grow or only grow slowly in time. In the latter case, the growth rate will decay with mesh refinement and a dissipative time integration method is likely to cancel the growth completely. However, for certain rare overlap parameters the instability becomes worse with mesh refinement. In these cases, the discretized interpolation problem has generalized eigenvalues.

Although weak, the spurious growth can cause problems in systems with different time scales, where there is a phenomenon which vary on a fast time scale (e.g. sound waves) mixed with a slow feature (e.g. Rossby waves). The computations, which usually are performed to capture a behavior on the slow scale, correspond to a very long time on the fast scale and thus the spurious growth can eventually destroy the numerical solution, cf. Browning et al. [2] and Olsson [7]. The weak spurious growth is also likely to be found in other problems where the solution must be computed for long times.

The spurious growth can be damped by adding an artificial second order difference term $\nu D_+ D_- u_j$ to the equation. To cancel the growth, it is sufficient with $\nu \sim O(h^2)$ when generalized eigenvalues are absent, but in their presence it is necessary to take $\nu \sim O(h)$. This makes the scheme only first order accurate with respect to the inviscid equation. To cure the accuracy problem, we can replace the second order dissipation term by the fourth order term $-\nu D_+^2 D_-^2 u_j$. It is found that this term damps the growing mode much more efficiently. Now, $\nu \sim O(h^3)$ is sufficient to cancel the spurious growth, even in the presence of generalized eigenvalues in the corresponding interpolation problem.

Is hard to foresee the implications of the present theory for hyperbolic problems in several space dimensions. We can expect there to be both "bad" and "good" overlaps in the domain and there can be a combination of damped and undamped disturbances present in the interior of the domain whose combined effect is difficult to predict. To further complicate the situation, an interpolation boundary can intersect a physical boundary so that the closest interpolation point is always only one grid point away from the physical boundary, regardless of the number of grid points in the interior. The experience from the two-dimensional calculations in [7] is that the accuracy of the method is degraded to first order when a second order dissipation of the type $\nu\Delta u$ is used, because the necessary amount of viscosity to damp the spurious growth is of the order $O(h)$. Preliminary computations with an improved version of that method indicates that the accuracy is restored when the second order dissipation is replaced by a forth order dissipation of the type $\nu\Delta^2 u$. These issues will be studied further in a forthcoming paper.

7 Acknowledgement

The authors would like to thank Prof. Heinz Kreiss for many interesting discussions on the present subject. FO was supported by the Swedish Institute for Pulp and Paper Research, Department of Energy through Los Alamos National Laboratory and Office of Naval Reserach grant N000014–J–1890. NAP was supported by Office of Naval Research grant N000014–J–1890.

References

[1] M. J. Berger. Stability of interfaces with mesh refinement. *Math. Comput.*, 45:301–318, 1985.

[2] G. Browning, J. J. Hack, and P. N. Swarztrauber. A comparison of three numerical methods for solving differential equations on the sphere. *Mon. Wea. Rev.*, 117:1058–1075, (1989).

[3] M. Ciment. Stable difference schemes with uneven mesh spacing. *Math. Comput.*, 25:219–227, 1971.

[4] M. Ciment. Stable matching of difference schemes. *SIAM J. Numer. Anal.*, 9:695–701, 1972.

[5] B. Gustafsson, H.-O. Kreiss, and J. Oliger. *Time dependent problems and difference methods.* In press, 1994.

[6] B. Gustafsson, H.-O. Kreiss, and A. Sundström. Stability theory of difference approximations for mixed initial boundary value problems. II. *Math. Comput.*, 26(119):649–686, 1972.

[7] F. Olsson. A solver for time dependent viscoelastic fluid flow. *J. Non-Newtonian Fluid Mech.*, 51:309–340, (1994).

[8] M. Paik. *On strict stability of difference approximations for hyperbolic initial-boundary value problems.* PhD thesis, University of California, Los Angeles, Department of Mathematics, UCLA, 90024 Los Angeles, 1995. In preparation.

[9] E. Pärt-Enander and B. Sjögreen. Conservative and non-conservative interpolation between overlapping grids for finite volume solutions of hyperbolic problems. *Comput. Fluids*, 23:551–574, (1994).

[10] L. G. M. Reyna. *Part III: On composite meshes.* PhD thesis, California Institute of Technology, Pasadena, California, 1982.

[11] G. Starius. On composite mesh difference methods for hyperbolic differential equations. *Numer. Math.*, 35:241–255, 1980.

[12] J. C. Strikwerda. Initial boundary value problems for the method of lines. *J. Comput. Phys.*, pages 94–107, 1980.

[13] L. N. Trefethen. Group velocity interpretation of the stability theory of Gustafsson, Kreiss and Sundström. *J. Comput. Phys.*, 49:199–217, 1983.